

Equilibrium Limit of Diffusion Equation for Interacting Particles: Are Bifurcations and Multiplicity of Correlation Functions an Artifact or Real?

G. L. Aranovich and M. D. Donohue*

Department of Chemical & Biomolecular Engineering, The Johns Hopkins University,
Baltimore, Maryland 21218

Received: January 18, 2007; In Final Form: March 5, 2007

The structure of a fluid is analyzed by taking the equilibrium limit of a diffusion equation including the Giacomini–Lebowitz term for intermolecular interactions. This equation represents the differential mass balance in fluids with the Metropolis algorithm for fluxes; it allows a new qualitative yet analytical approximation for the direct correlation function over the entire range of fluid densities and temperatures. This approximation is analogous to a classical Ono–Kondo model for adsorption if the distribution of molecules around a central molecule is viewed as the adsorption of molecules on a central molecule. While this model qualitatively predicts known behavior for both gas and liquid phases, approaching a phase transition (e.g., condensation of gas into liquid) results in a bifurcation and multiplicity of the direct correlation function. The model predicts a sequence in the transformation of correlation functions from that of a gas to that of a liquid. This sequence starts with the appearance of an isolated loop in the direct correlation function, indicating states that are stable but cannot be achieved without perturbation of the system. However, the system seems to sense its proximity to a phase transition and reflects the distance to the phase boundary by the size and shape of this isolated loop in the direct correlation function. At lower temperatures, this loop merges with the gas-phase peak, indicating that clusters can form spontaneously. Then, these clusters grow into a high-density (liquid) phase. The notion of bifurcations and multiplicity in correlation functions is an unusual and controversial concept. Certainly, it is unexpected and raises important questions: (a) if such a behavior is not real, why does the diffusion equation predict such behavior, i.e., is it a mathematical artifact or is it due to conflicting physical assumptions? (b) if this behavior is real, how does one interpret it at a molecular level? Here, we present some interpretations, but they are open for discussion.

1. Introduction

The correlation and radial distribution functions play a key role in the statistical mechanics of fluids.^{1–3} These functions give important information about the molecular structure of a fluid and determine the thermodynamic behavior of the system.²

There are numerous approaches to studying the molecular structure of fluids. Fundamental insights into intermolecular correlations and distribution functions have come from classical integral equations, including the Ornstein–Zernike equation^{4–7}

$$g(r_{12}) - 1 = c(r_{12}) + \rho_{\infty} \int c(r_{13})[g(r_{23}) - 1] d\vec{r}_3 \quad (1)$$

where $g(r)$ is the pair distribution function, $c(r)$ is the direct correlation function, ρ_{∞} is the reduced bulk density, r_{12} and r_{13} are the distances between molecule 1 and molecules 2 and 3, respectively, and \vec{r}_3 is radius vector from the central molecule (molecule 1) to molecule 3. The density distribution around a central molecule, $\rho(r)$, is

$$\rho(r) = \rho_{\infty} g(r) \quad (2)$$

The Ornstein–Zernike eq 1 divides the total correlation function, $h(r_{12}) = g(r_{12}) - 1$, into two parts, a direct part and an indirect part. This equation can be considered as a definition of the direct correlation function or a relation between functions

$g(r)$ and $c(r)$.² If $c(r)$ is given in terms of $g(r)$, the Ornstein–Zernike equation would give a closed integral equation for $g(r)$. Classical theories have developed various approximations for closed integral equations (such as Percus–Yevick⁸ and hypernetted-chain equations⁹) and resulted in a variety of approaches and applications for complex systems.^{10–14}

Solving integral equations with respect to correlation functions is not a simple problem—there are no simple analytical solutions and even numerical calculations can be difficult.³ Additional difficulties arise in the proximity of phase transitions and in the two-phase region where multiple solutions can be expected. It is well-known that nonlinear algebraic equations require special numerical techniques for regions of multiple solutions^{15,16} because standard algorithms (such as successive substitutions and the Newton–Raphson method) diverge; this is especially true for more complex (integral) equations where mathematical methods have not been developed for systems with multiple solutions. Though multiplicity of solutions at phase transitions (ref 3, Chapter 3) and bifurcations of density distributions and order parameters are known in principle (in particular, for liquid–solid transitions¹⁷ and for phase transitions in dimers¹⁸), mathematical difficulties have prevented rigorous and comprehensive studies of such cases.

The goal of this paper is to examine bifurcations and multiplicity in the direct correlation functions of fluids. To do this, we consider the equilibrium limit of a diffusion equation with the Giacomini–Lebowitz^{20–22} (“mobility”) term for inter-

* Corresponding author. E-mail: mdd@jhu.edu.

molecular interactions. This equation can be derived as a differential mass balance in fluids with density functionals using the Metropolis algorithm for fluxes.¹⁹ It allows analytical solutions for direct correlation functions over the entire range of densities and temperatures and predicts bifurcations and multiple solutions.

In previous publications,^{23–26} we have analyzed Ono–Kondo-like^{27,28} density functionals around the central molecule in mean-field and beyond mean-field approximations; however, these calculations did not study correlation and density distribution functions. In a famous review on the theory of phase equilibrium in fluids,²⁹ Widom writes that “modern” era calculations going beyond mean-field are an “important activity, but where one seeks qualitative understanding rather than quantitative accuracy, the mean-field theory remains an indispensable tool”. In this paper, we seek such a qualitative understanding of multiple solutions and bifurcations in the direct correlation function.

2. Diffusion Equation for Interacting Particles

Giacomin and Lebowitz (GL)^{20,21} proposed a theory for the time evolution of the density distribution, $\rho(\vec{r}, t)$, in systems with interacting particles. This approach was developed to predict the macroscopic evolution of systems with short- and long-range interactions.²² In GL theory, in the hydrodynamic limit, the contribution of interactions to the diffusion flux, ΔF , is $\Delta F = \sigma \nabla H$, where H is the configurational energy and $\sigma = \rho(1 - \rho)$ is called the “mobility”. Note that dimensionless density, ρ , is a convenient variable widely used in classical theories of equations of state for fluids.^{2,30} In particular, for spherically symmetric molecules, ρ can be defined as $(\pi/6)nd^3$, where n is number of molecules per unit of volume and d is a parameter characterizing the size of the molecule (for hard spheres, it is diameter, for Lennard-Jones molecules, it is σ , etc.).

The diffusion equation for fluids with the “mobility” term can be written as:^{19–22}

$$\frac{\partial \rho}{\partial t} = \nabla \{ D [\nabla \rho + \rho(1 - \rho) \nabla H] \} \quad (3)$$

where D is the diffusion coefficient. This equation represents a differential mass balance in fluids where density functionals for fluxes are defined by the Metropolis algorithm. As shown in ref 19–22, eq 3 is able to describe diffusion between coexisting phases and, in the limit of equilibrium, it predicts a (mean-field) phase diagram. (An illustrative way of deriving the diffusion equation with the “mobility” term is presented in the Appendix.)

Here, we will show that the diffusion equation for interacting particles can predict bifurcations for the direct correlation function and multiple solutions for coexisting and metastable phases. Consider diffusion in a molecular system where a central molecule is at the coordinate origin and other molecules diffuse in the space around it (Figure 1). In terms of the diffusion equation, the central molecule imposes an external field on surrounding molecules. At the same time, surrounding molecules interact with each other. The density distribution around the central molecule determines the pair correlation function for the molecular system. This distribution can be calculated from eq 3. However, the exact equation for the configurational energy is not available; therefore, we will use a significant simplification: only direct correlations with surrounding molecules and with the central molecule will be taken into account. Therefore, the resulting density distribution will represent the direct correlation function, not the (full) pair correlation function.

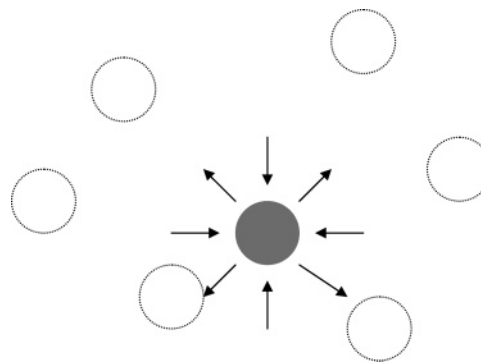


Figure 1. Diffusion of interacting molecules around the central molecule (dark circle). At equilibrium, the fluxes to and from the central molecule compensate each other.

The direct correlation function still captures the features that we want to discuss in this paper: bifurcations and multiple solutions near phase boundaries. To our knowledge, these features have not been analyzed previously because of mathematical difficulties when using classical methods; however, using the diffusion eq 3 allows circumventing these difficulties and, hence, demonstrating bifurcations and multiplicity.

We understand that our approach relies on significant simplifications compared to rigorous methods, including classical integral equations.^{2–9} However, it shows new and unusual aspects of correlation functions, bifurcations, and multiplicity, which can expand the scope of applications for rigorous methods and stimulate more sophisticated analyses. At the same time, it raises important questions: whether such behavior is real and how it can be interpreted at a molecular level.

3. Approximation for Spherically Symmetric Interactions

Consider a system of molecules with spherically symmetric interactions. It follows from eq 1, if correlations through a third molecule do not exist, $c(r) = g(r) - 1$. For this case (no indirect correlations), solution of eq 3 gives $\rho(r)$ which is related to $c(r)$ as

$$\rho(r) = \rho_{\infty} [c(r) + 1] \quad (4)$$

The function $\rho_{\infty} [c(r) + 1]$ is the density distribution around a central molecule without indirect correlations. This function becomes the full density distribution, $\rho_{\infty} g(r)$, if $c(r)$ is substituted by $g(r) - 1$, although calculation of $g(r)$ goes beyond our consideration.

To consider direct correlations, the configurational energy can be written as the total potential energy for interaction of a probe molecule (a) with the central molecule, (b) with the nearest neighbors, and (c) with other molecules in the following form:

$$H = \frac{\varphi(r)}{kT} + \frac{z\epsilon}{kT} \rho(r) + \frac{U_0}{kT} \quad (5)$$

where $\varphi(r)$ is the energy of interaction with the central molecule (potential function, such as Lennard-Jones), ϵ is the energy of interaction with nearest neighbors, U_0 is the energy of interaction with all other molecules, z is the coordination number (defined for fluids as $\int_0^d n g(r) 4\pi r^2 dr$; see ref 31, p 71), k is Boltzmann’s constant, and T is the absolute temperature. Here, we will assume that U_0 does not depend on r significantly; so the gradient of H is determined primarily by $\varphi(r)/kT$ and $z\epsilon/kT \rho(r)$.

In eq 5, the term $z\epsilon/kT \rho(r)$ is the mean-field energy of interactions without correlations,^{23–28} therefore, eq 5 gives the potential energy without indirect correlations.

Consider steady-state conditions by imposing $\partial\rho/\partial t = 0$ in eq 3. Then, using eq 5 and neglecting $\partial U_0/\partial r$, eq 3 can be written in spherical coordinates:

$$\frac{\partial}{\partial r} \left[D \frac{\partial \rho}{\partial r} + \frac{D\rho(1-\rho)}{kT} \frac{\partial \varphi}{\partial r} + D\rho(1-\rho) \frac{z\epsilon}{kT} \frac{\partial \rho}{\partial r} \right] = 0 \quad (6)$$

which gives:

$$\frac{\partial \rho}{\partial r} + \frac{\rho(1-\rho)}{kT} \frac{\partial \varphi}{\partial r} + \rho(1-\rho) \frac{z\epsilon}{kT} \frac{\partial \rho}{\partial r} = \text{Const} \quad (7)$$

The constant of integration in eq 7 defines a flux in the radial direction (to/from the central molecule).¹⁹ At equilibrium, this $\text{Const} = 0$ and eq 7 can be represented in the following form:

$$\frac{\partial \left(\ln \frac{\rho}{1-\rho} + \frac{z\epsilon}{kT} \rho \right)}{\partial r} = - \frac{1}{kT} \frac{\partial \varphi}{\partial r} \quad (8)$$

After integration, eq 8 gives

$$\ln \frac{\rho}{1-\rho} + \frac{z\epsilon}{kT} \rho + \frac{\varphi}{kT} = A \quad (9)$$

where A is a constant of integration. Because $\varphi \rightarrow 0$ as $r \rightarrow \infty$, then this constant is

$$A = \ln \frac{\rho_\infty}{1-\rho_\infty} + \frac{z\epsilon}{kT} \rho_\infty \quad (10)$$

Here we assume that $\varphi(r)$ is the Lennard-Jones potential function with an energetic parameter of ϵ in eq 5; this is because nearest neighbors are at (or near) the minimum of $\varphi(r)$. Then, combining eqs 9 and 10 gives:

$$\ln \frac{\rho(1-\rho_\infty)}{(1-\rho)\rho_\infty} + \frac{z\epsilon}{kT} (\rho - \rho_\infty) + \frac{4\epsilon}{kT} \left[\left(\frac{\sigma}{r} \right)^6 - \left(\frac{\sigma}{r} \right)^{12} \right] = 0 \quad (11)$$

4. Thermodynamic Basis of Equation 11 and Analogy with Ono–Kondo Model

Equation 11 describes the density distribution around a central molecule. This equation results from solving the diffusion eq 3 for a spherically symmetric H given by approximation (eq 5) and zero flux to/from the central molecule. (As mentioned previously, details on the derivation of diffusion equation with GL “mobility” term can be found in ref 19–22).

The physics predicted by eq 11 can be illustrated by viewing a distribution of molecules around a central molecule as the adsorption of molecules surrounding a central molecule. The classical Ono–Kondo theory of adsorption^{27,28} and its modern versions^{23–26} give the following form for equation of equilibrium:

$$\ln \frac{\rho(1-\rho_\infty)}{(1-\rho)\rho_\infty} + \frac{\varphi_A}{kT} + \frac{\varphi^*}{kT} - \frac{z\epsilon}{kT} \rho_\infty = 0 \quad (12)$$

where φ_A is the energy of interaction between an adsorbate molecule and adsorbent, φ^* is the energy of interaction between an adsorbate molecule and surrounding molecules, and $\ln \rho(1-\rho_\infty)/(1-\rho)\rho_\infty$ is the entropy term. Ono–Kondo-like equations give density distributions near surfaces and predict multiple

solutions in ranges of phase transitions.¹⁶ If $\varphi^* = z\epsilon\rho$ and $\varphi_A = 4\epsilon[(\sigma/r)^6 - (\sigma/r)^{12}]$, eq 12 reduces mathematically to eq 11. This analogy allows considering the central molecule as an adsorbent and surrounding molecules as an adsorbate.

This analogy to the adsorption of molecules on a central molecule has profound conceptual roots. In Ono–Kondo adsorption theory, the free energy is represented as a functional of the density distribution and eq 12 results from minimizing this functional. Equation 11 results from writing the fluxes (to and from the central molecule) as functionals of the density distribution and setting these fluxes equal to each other (i.e., zero net flux).

Note that lattice versions of Ono–Kondo theory describe multilayer adsorption and multiple solutions show densities of coexisting phases in adsorbed layers. Equation 11 is not constrained to be on a lattice; however, as demonstrated later, it also predicts multiple distributions of densities around the central molecule for coexisting phases. In the limit of small densities, eq 11 results in $\rho = \rho_\infty \exp\{-4\epsilon/kT [(\sigma/r)^6 - (\sigma/r)^{12}]\}$; combining this with eq 4 gives $c(r) = \exp\{-4\epsilon/kT [(\sigma/r)^6 - (\sigma/r)^{12}]\} - 1$, which coincides with the elementary classical approximation for $c(r)$.³¹

5. Exact Analytical Solutions of Equation 11

Equation 11 allows (remarkably simple) exact analytical solutions of r as a function of ρ . This can be seen if eq 11 is rewritten in the form of the following quadratic equation:

$$qy^2 + y - 1 = 0 \quad (13)$$

where $y = (r/\sigma)^6$ and $q = kT/4\epsilon \ln(\rho(1-\rho_\infty)/(1-\rho)\rho_\infty) + z/4(\rho - \rho_\infty)$. Solutions of eq 13 are $y_{1,2} = (-1 \pm (1+4q)^{1/2})/2q$, which after algebraic manipulations, gives:

$$r = \sigma \left[\frac{-1 \pm (1+4q)^{1/2}}{2q} \right]^{1/6} \quad (14)$$

Note that the exact analytical solution (eq 14) is possible due to a specific form of Lennard-Jones (LJ) potential function (quadratic with respect to $1/y$). However, the existence of bifurcations is not limited by the choice of the LJ potential: any function, $f(1/y)$, giving multiple solutions to equation $f(1/y) = q$ results in bifurcations. Analysis of non-LJ potential functions (including various polar and non-radial terms with angular coordinates) would be interesting, but this goes beyond the scope of the present paper.

As mentioned previously, $\rho(r) = \rho_\infty [c(r) + 1]$ is the density distribution around a central molecule without indirect correlations. Therefore, eq 14 allows plotting $\rho_\infty [c(r) + 1]$ as a function of r .

Figure 2 shows $\rho(r) = \rho_\infty [c(r) + 1]$ predicted by eq 14 at $\epsilon/kT = -0.37$, $z = 12$, and $\rho_\infty = 0.1$. As shown in Figure 2, in this case the behavior of $\rho(r) = \rho_\infty [c(r) + 1]$ is classical; it goes up to a maximum at $r = \sigma 2^{1/6}$; then it goes down and approaches ρ_∞ asymptotically.

6. Bifurcations and Multiplicity

Figure 3 shows $\rho_\infty [c(r) + 1]$ as a function of r predicted by equation 14 at $\epsilon/kT = -0.373$, $z = 12$, and $\rho_\infty = 0.1$. As shown in Figure 3, there is a significant change compared to Figure 2; there are multiple solutions in the range of r around 1.1σ which is seen as an isolated ellipse above the gas-phase peak. In Figure 4, where $\epsilon/kT = -0.39$ and the other parameters are the same as in Figure 3, this ellipse becomes larger and elongates

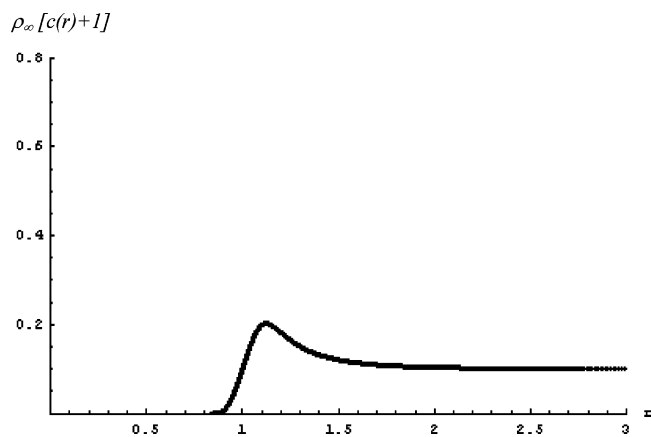


Figure 2. Dependence of $\rho_\infty [c(r) + 1]$ on r predicted by eq 14 at $\epsilon/kT = -0.37$, $z = 12$, and $\rho_\infty = 0.1$. Here r is in units of σ .

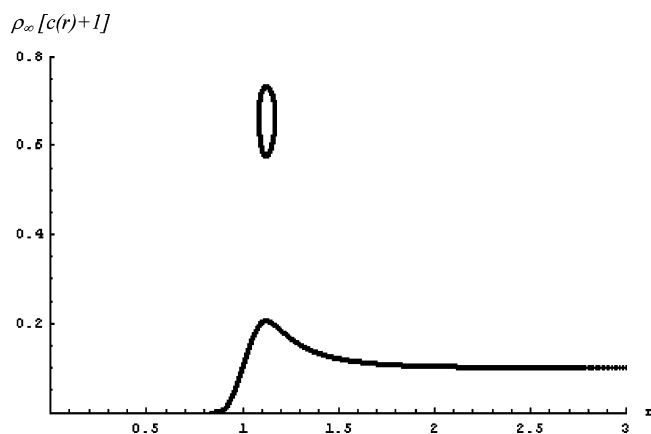


Figure 3. Dependence of $\rho_\infty [c(r) + 1]$ on r predicted by eq 14 at $\epsilon/kT = -0.373$, $z = 12$, and $\rho_\infty = 0.1$. Here r is in units of σ .

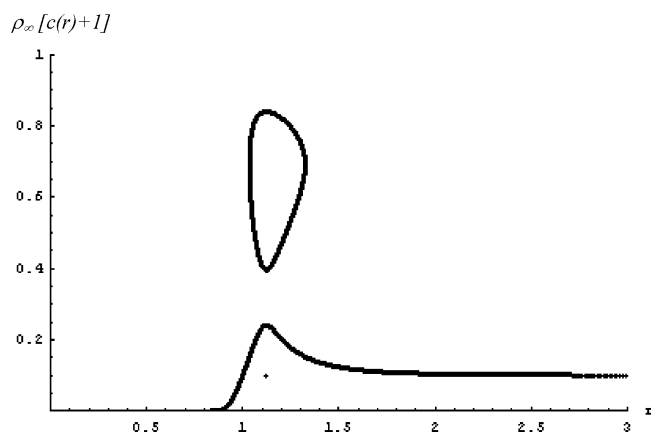


Figure 4. Dependence of $\rho_\infty [c(r) + 1]$ on r predicted by eq 14 at $\epsilon/kT = -0.39$, $z = 12$, and $\rho_\infty = 0.1$. Here r is in units of σ .

vertically. In Figure 5 with $\epsilon/kT = -0.4$, the lower tip of the ellipse merges with the gas-phase peak. This ellipse represents a possible set of states where there can be a high-density cluster around the central molecule. We believe that while this part of the distribution function is isolated, the cluster cannot form unless the system is perturbed, but when the isolated part merges with the gas-phase peak, the cluster can form spontaneously. (However, it should be emphasized that we are discussing the thermodynamics, not the kinetics, of cluster formation.)

As shown by Figure 5, values of $\rho_\infty [c(r) + 1]$ can reach 0.9 which gives $c(r)$ about 9. This represents the formation of a cluster and reflects the fact that, in a dense cluster, direct

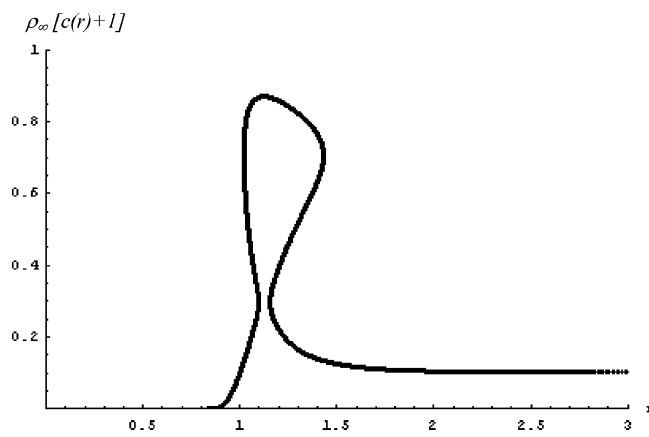


Figure 5. Dependence of $\rho_\infty [c(r) + 1]$ on r predicted by eq 14 at $\epsilon/kT = -0.4$, $z = 12$, and $\rho_\infty = 0.1$. Here r is in units of σ .

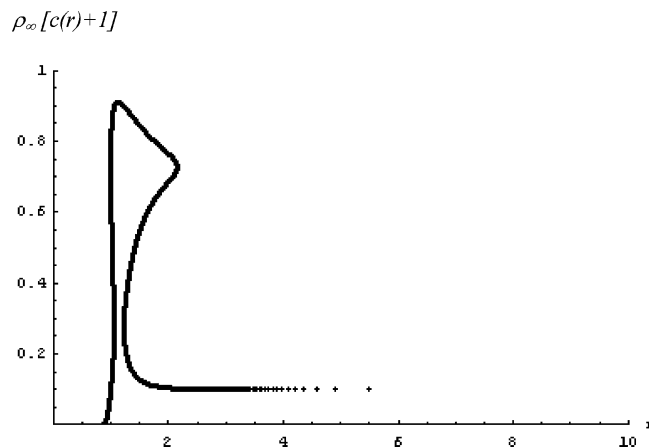


Figure 6. Dependence of $\rho_\infty [c(r) + 1]$ on r predicted by eq 14 at $\epsilon/kT = -0.42$, $z = 12$, and $\rho_\infty = 0.1$. Here r is in units of σ .

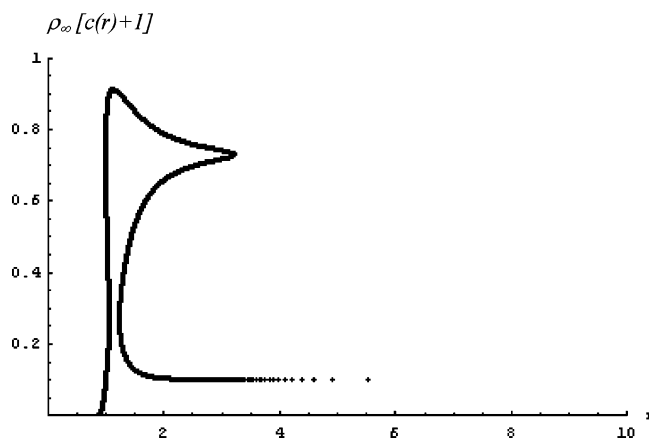


Figure 7. Dependence of $\rho_\infty [c(r) + 1]$ on r predicted by eq 14 at $\epsilon/kT = -0.422$, $z = 12$, and $\rho_\infty = 0.1$. Here r is in units of σ .

correlations with the central molecule indicate many nearest neighbors. In fact, for dense clusters in equilibrium with a gas phase, $c(r)$ can be up to z . Note that such large values of $c(r)$ seem to occur only in ranges of multiplicity and are not observed in classical solutions,² i.e., classical solutions do not predict cluster formation or the onset of a phase transition.

Figures 6–9 show $\rho_\infty [c(r) + 1]$ as a function of r predicted by equation 14 at $z = 12$, $\rho_\infty = 0.1$, and ϵ/kT changing from -0.42 to -0.4223 . As shown in Figures 6–9, this small change of ϵ/kT results in horizontal elongation of the initially isolated ellipse. This corresponds to growing the high-density cluster around the central molecule. At $\epsilon/kT = -0.4223$ (Figure 9),

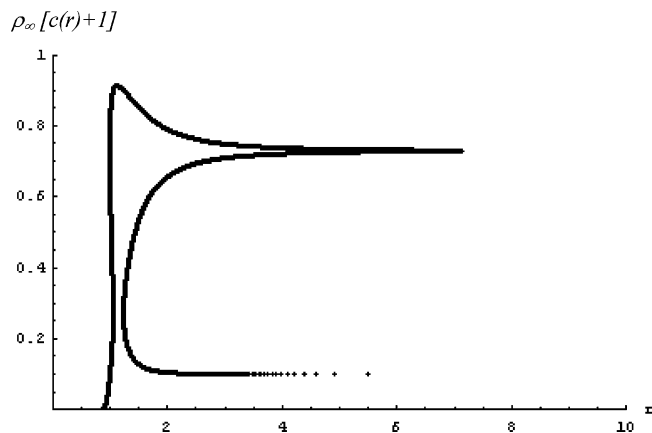


Figure 8. Dependence of $\rho_\infty [c(r) + 1]$ on r predicted by eq 14 at $\epsilon/kT = -0.4222$, $z = 12$, and $\rho_\infty = 0.1$. Here r is in units of σ .

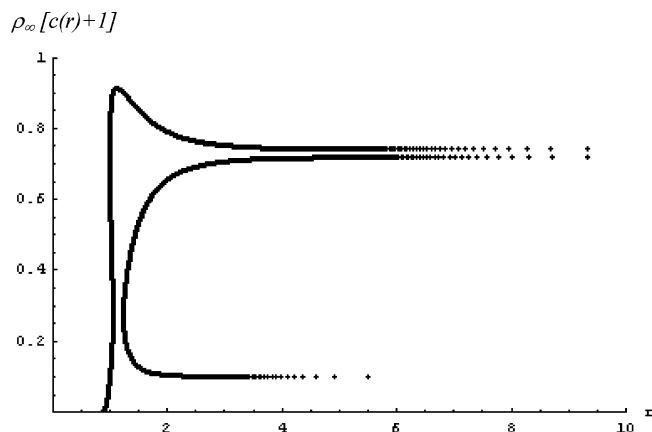


Figure 9. Dependence of $\rho_\infty [c(r) + 1]$ on r predicted by eq 14 at $\epsilon/kT = -0.4223$, $z = 12$, and $\rho_\infty = 0.1$. Here r is in units of σ .

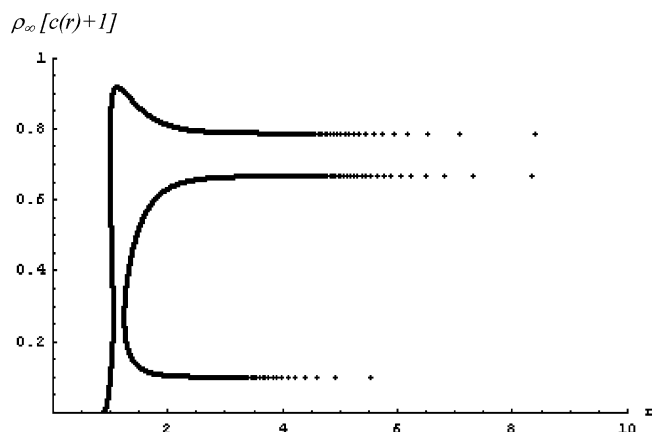


Figure 10. Dependence of $\rho_\infty [c(r) + 1]$ on r predicted by eq 14 at $\epsilon/kT = -0.425$, $z = 12$, and $\rho_\infty = 0.1$. Here r is in units of σ .

this cluster reaches infinity, which indicates the existence of a macroscopic liquid phase in equilibrium with the vapor.

Figures 2–9 show how $\rho(r)$ for a gas (Figure 1) transforms into $\rho(r)$ for a liquid (Figure 9) as the temperature decreases and gas condenses into liquid. This transformation goes through several intermediate steps: (a) the appearance and growth of clusters that may be formed by a perturbation to the system (Figures 3, 4); (b) turning this precursor into a cluster that can form spontaneously (Figure 5); and (c) growing the spontaneous cluster to infinite size (Figures 6–9).

Figures 10 and 11 show further changes as the temperature continues to decrease. In Figure 10, $\epsilon/kT = -0.425$; in Figure

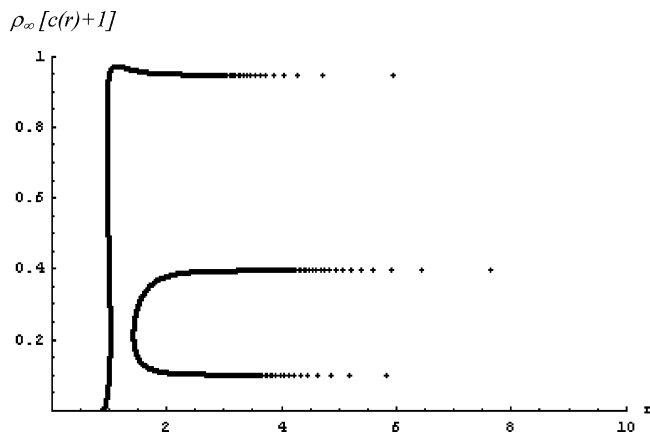


Figure 11. Dependence of $\rho_\infty [c(r) + 1]$ on r predicted by eq 14 at $\epsilon/kT = -0.5$, $z = 12$, and $\rho_\infty = 0.1$. Here r is in units of σ .

11, $\epsilon/kT = -0.5$; all other parameters in Figures 10 and 11 are the same as in Figures 2–9.

Figure 12 shows $\rho_\infty [c(r) + 1]$ as a function of r predicted by eq 14 at $z = 12$, $\rho_\infty = 0.02$, and various ϵ/kT : -0.55 (a), -0.56 (b), -0.563 (c), -0.5633 (d), -0.564 (e), -0.8 (f), -0.9 (g), and -1.0 (h). As shown in Figure 12, at $\rho_\infty = 0.02$, there is a different sequence of events: the isolated ellipse grows horizontally first (reaching infinity at $\epsilon/kT \approx -0.5633$), then it grows vertically toward the gas-phase peak until it merges with this peak.

7. Phase Diagram and the Critical Point

Figures 2–12 illustrate the behavior of a fluid near the point of phase transition from solutions to eq 3. These solutions have several special features, including the potential for clusters which can be formed by perturbation, conditions where these precursors turn into spontaneously formed clusters, and conditions where the size of the clusters diverges to infinity. These conditions form lines on the phase diagram and can be identified from eq 14.

From eq 7, at $Const = 0$ (equilibrium), it follows that

$$\frac{\partial \rho}{\partial r} = - \frac{\rho(1 - \rho)}{kT + \rho(1 - \rho)z\epsilon} \frac{\partial \varphi}{\partial r} \quad (15)$$

As seen from eq 15, $\partial \rho / \partial r$ goes to infinity as

$$kT + \rho(1 - \rho)z\epsilon = 0 \quad (16)$$

which is the well-known mean-field equation for a spinodal.¹

The first appearance of isolated ellipses above the gas-phase peak can be identified by simultaneous solution of eqs 16 and 11, where the term $4\epsilon/kT[(\sigma/r)^6 - (\sigma/r)^{12}]$ is substituted by its value at $r = \sigma 2^{1/6}$, which is ϵ/kT .

As seen from eq 14, $r \rightarrow \infty$ when q (defined by eq 14) goes to zero. Note that it is possible that $r \rightarrow \infty$, but $\rho \rightarrow \rho^*$ and $\rho^* \neq \rho_\infty$. Figure 13 shows the phase diagram calculated from solutions of eq 3 with the configurational energy given by eq 5. In Figure 13, line “a” indicates the appearance of the isolated parts in density distributions. Line “b” in this figure represents points where isolated parts become connected to the gas-phase peak and precursors turn into clusters that can be formed spontaneously. Lines “c” and “d” are the classical mean-field binodal and spinodal. Analysis of solutions illustrated in Figures 2–12 shows that line “c” represents points where the cluster sizes diverge to infinity; line “d” represents points

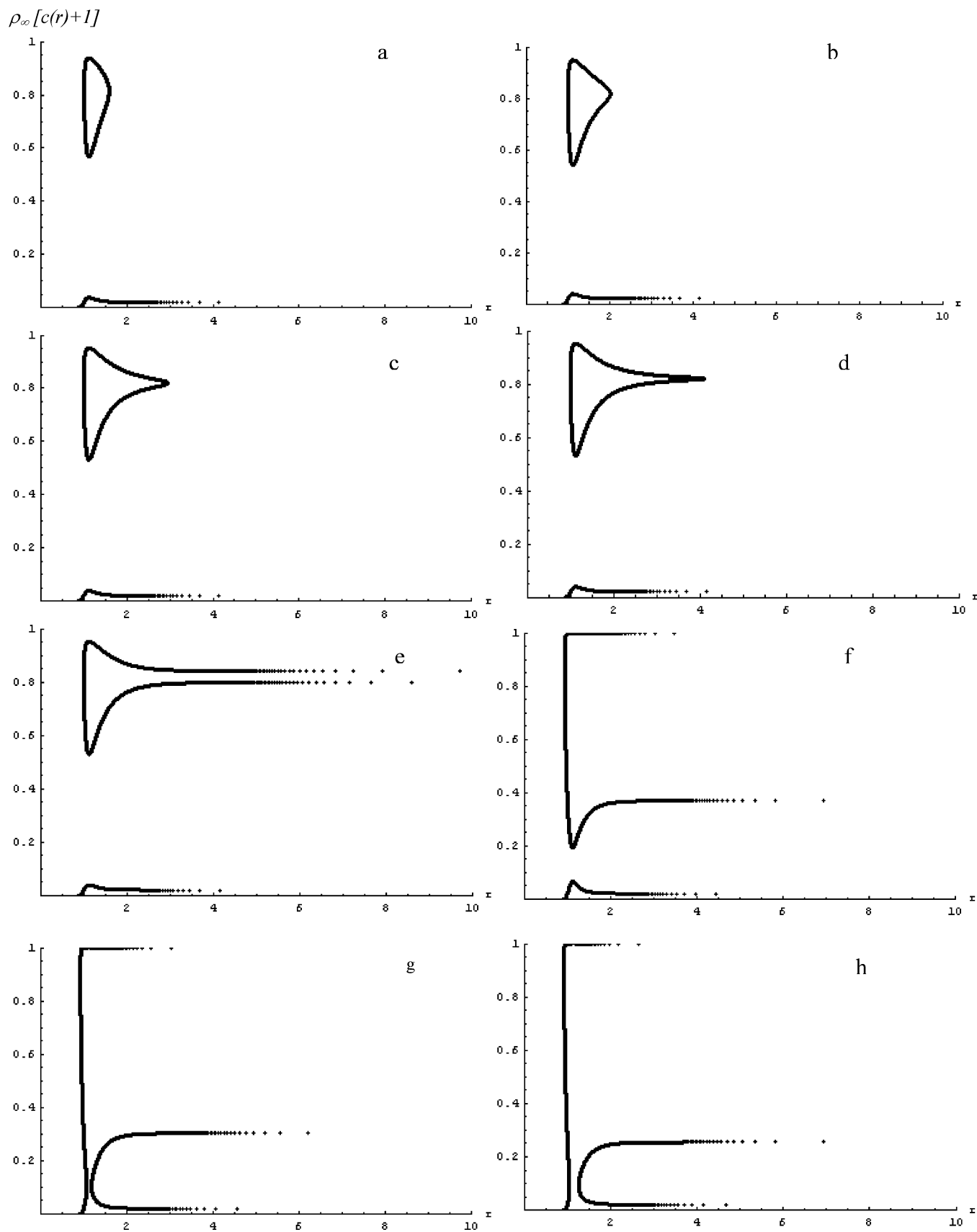


Figure 12. Dependence of $\rho_{\infty}[c(r)+1]$ on r predicted by eq 14 at $z = 12$, $\rho_{\infty} = 0.02$, and various ϵ/kT : -0.55 (a), -0.56 (b), -0.563 (c), -0.5633 (d), -0.564 (e), -0.8 (f), -0.9 (g), and -1.0 (h). Here r is in units of σ .

where the unstable branch and initial gas-phase line merge—this is illustrated in Figure 14 at $\epsilon/kT = -0.9$, $z = 12$, and $\rho_{\infty} = 0.1$.

Figures 15 and 16 show the behavior of $\rho(r)$ near the critical point. Figure 15 gives distributions by approaching the critical point from above, and Figure 16 shows the changes of $\rho(r)$ by

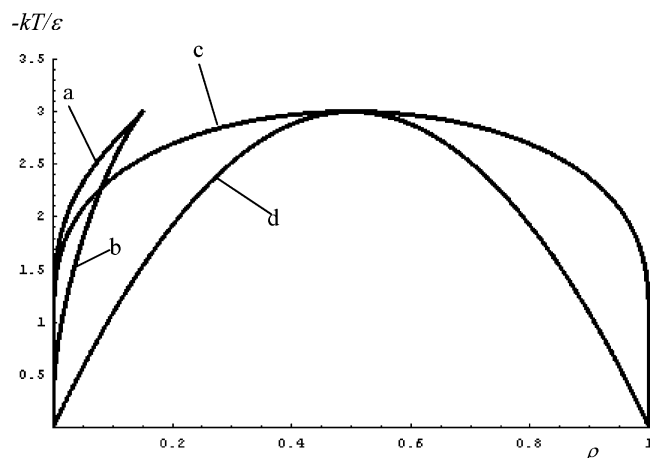


Figure 13. Phase diagram predicted from equilibrium limit of diffusion equation. Line “a” indicates appearance of isolated parts in density distributions (precursors). Line “b” is points where isolated parts become connected to the gas-phase peak and precursors turn into spontaneous clusters. Lines “c” and “d” are spinodal and binodal respectively.

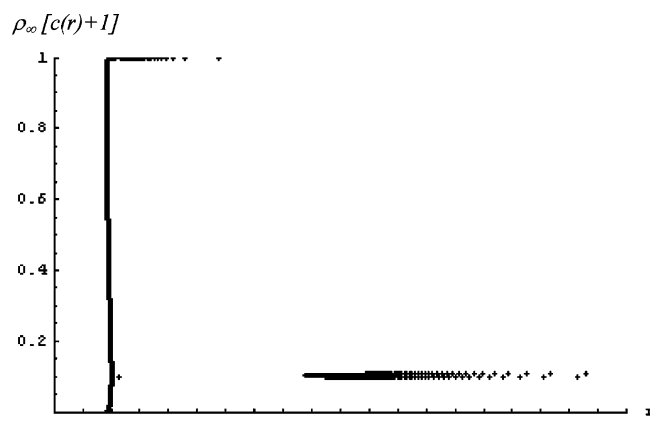


Figure 14. Dependence of $\rho_{\infty} [c(r) + 1]$ on r predicted by eq 14 at $\epsilon/kT = -0.9$, $z = 12$, and $\rho_{\infty} = 0.1$. Here r is in units of σ .

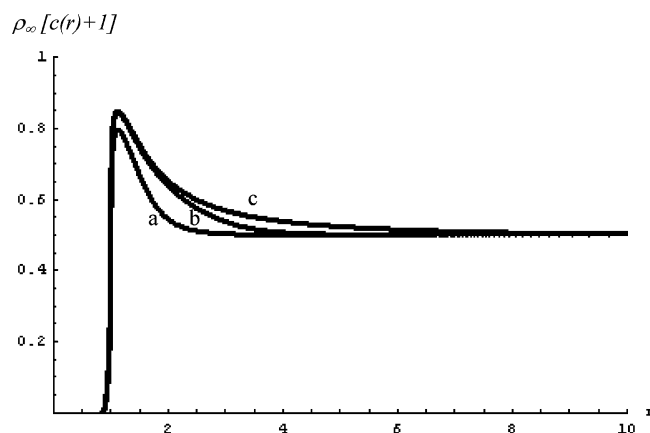


Figure 15. Dependence of $\rho_{\infty} [c(r) + 1]$ on r predicted by eq 14 at $z = 12$, $\rho_{\infty} = 0.5$, and various ϵ/kT : -0.3 (a), -0.33 (b), and -0.3333 (c). Here r is in units of σ .

approaching the critical point from below. As shown by these Figures, the changes are smooth (continuous) when approaching from above and discontinuous when approaching from below: there is no multiplicity in the critical point, but any small decrease of temperature results in (discontinuous) appearance of multiplicity.

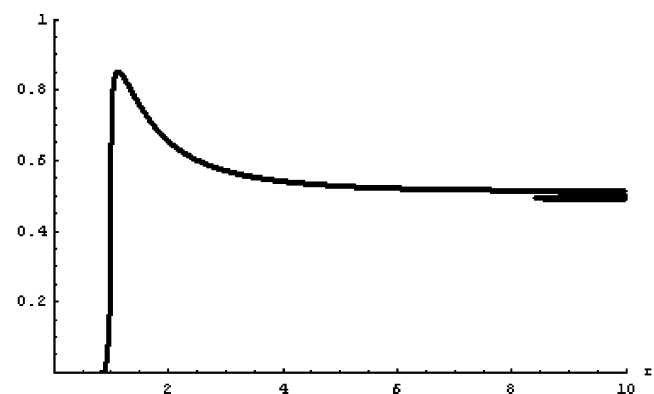
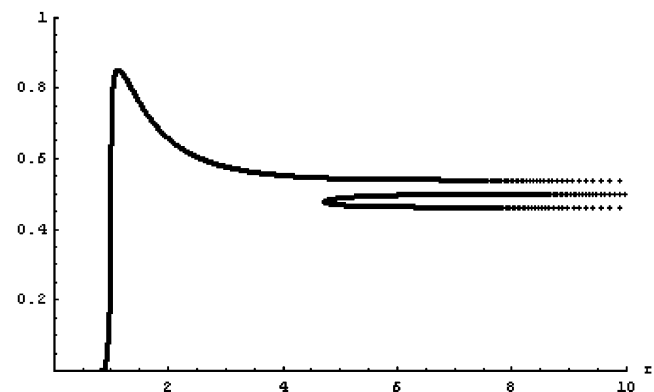
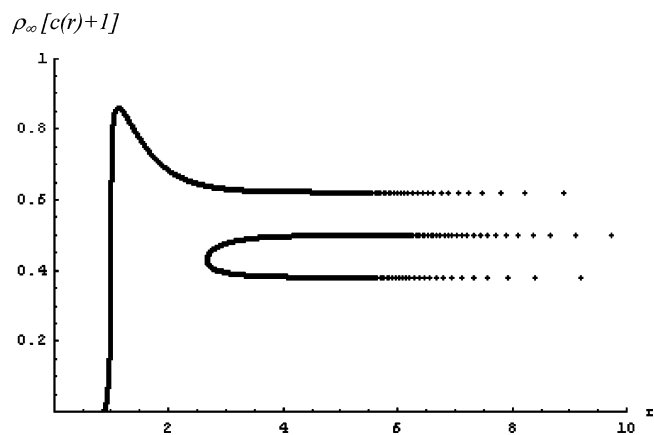


Figure 16. Dependence of $\rho_{\infty} [c(r) + 1]$ on r predicted by eq 14 at $z = 12$, $\rho_{\infty} = 0.5$, and various ϵ/kT : -0.34 (a), -0.334 (b), and -0.3334 (c). Here r is in units of σ .

Note that the behavior of clusters around a central molecule illustrated in Figures 2–16 is analogous to that of a two-dimensional phase in equilibrium with three-dimensional one.³² This is because phase transitions in lower-dimensional phases result in bifurcations and multiple solutions for correlation functions.

8. Discussion

Classical theories of pair correlation functions consider a central molecule as belonging to a certain phase (e.g., gas or liquid).^{1–4} Therefore, correlation functions and density distributions do not have bifurcations and multiplicity. However, going through a phase transition (e.g., condensing gas into liquid) should result in a transition of the density distribution around a central molecule from gas-like to liquid-like. This transition is not just crossing certain line on a phase diagram—there can be a complex sequence of changes including nucleation and

growing clusters. However, such a transition has not been analyzed in terms of density distributions around a central molecule.

Theories of the density distributions are limited to one-phase regions, but nucleation theory is applicable only in two- (multi-) phase regions. In this regard, our results might be viewed as a bridge between these two approaches.

As shown in Figures 2–16, crossing phase boundary starts with precursors, isolated parts in density distributions (with multiple solutions for $\rho(r)$). These isolated parts allow clusters around a central molecule. These clusters may be formed spontaneously or with a perturbation of the system (such as quenching). There is a critical size of clusters, which is followed by formation of a new phase.

Modern approaches use rigorous theories of phase transitions for complex systems.^{10–14} However, even for the simplest systems, the very definitions of phase and phase transition have unresolved and controversial aspects. Even though the concept of phases is widely used, it is not easy to define precisely. This is a well-known problem reflected in various discussions on phase equilibria.²⁹ In particular, a phase is a region in the parameter space of thermodynamic variables in which the free energy is analytic. When a system goes from one phase to another, there will generally be a stage where the free energy is nonanalytic. This is a phase transition.

However, the existence of the liquid–gas critical point reveals a slight ambiguity in such definitions. When going from the liquid to the gaseous phase, one usually crosses the phase boundary, but it is possible to choose a path that never crosses the boundary by going around the critical point. Thus, phases can sometimes blend continuously into each other.

Note that the free energy is a functional of $\rho(r)$ including terms like $\int_0^\infty \rho(r)\varphi(r)4\pi r^2 dr$ (ref 1, page 189). Therefore, discontinuities or bifurcations of $\rho(r)$ do not necessarily translate into nonanalytical behavior of the free energy, and the concept of phase transition as a bifurcation of $\rho(r)$ can help to overcome the (above-mentioned) ambiguity in the definition of a phase transition for systems with critical points.

As mentioned previously, bifurcations and multiplicity of density distributions are known for liquid–solid transitions.¹⁷ For gas–liquid transitions, we are not aware of any publications showing bifurcations and multiplicity. In our opinion, the reasons for this are the mathematical difficulties in getting analytical solutions in rigorous theories and problems in simulations near phase transitions and at multiphase conditions.

Conceptually, the results predicted by eq 3 at the equilibrium limit and illustrated in Figures 2–16 are reasonable in terms of the molecular behavior at phase transitions. Transformation from a gas-like $\rho(r)$ to a liquid-like distribution requires intermediate states—precursors and clusters that can grow into the new phase. This sequence of events does not contradict existing concepts or theories of the gas–liquid transition.

We understand that bifurcations and multiplicity of correlation functions are unusual and controversial concepts. Even semantically, there is a contradiction between “multiplicity” and “function”, which is defined mathematically as single-valued. On the other hand, statistical physics does not give a proof that $\rho(r)$ is always single-valued and that “correlation function” is defined as a function in the mathematical sense (i.e., single-valued by definition). Hence, these results raise important questions: (1) If such a behavior is not real, why does the diffusion equation predict such behavior, i.e., is it a mathematical artifact or is it due to conflicting physical assumptions? (2) If this behavior is real, how does one interpret it at a molecular

level? Here, we presented some interpretations, but they are open for discussion.

Appendix

Illustrative Derivation of Equation 3 by Considering Functionals for Fluxes Using Metropolis Algorithm. At $D = \text{Const}$, classical diffusion equation for noninteracting particles is

$$\frac{1}{D} \frac{\partial \rho}{\partial t} = \frac{\partial^2 \rho}{\partial x^2} + \frac{\partial^2 \rho}{\partial y^2} + \frac{\partial^2 \rho}{\partial z^2} \quad (17)$$

Generalization for interacting particles can be written as

$$\frac{1}{D} \frac{\partial \rho}{\partial t} = \Psi \left[\frac{\partial^2 \rho}{\partial x^2}, \frac{\partial^2 \rho}{\partial y^2}, \frac{\partial^2 \rho}{\partial z^2}, \frac{\partial \rho}{\partial x}, \frac{\partial \rho}{\partial y}, \frac{\partial \rho}{\partial z}, \rho \right] \quad (18)$$

where ψ is an unknown operator (reflecting mechanisms of interactions).

Equation 18 can be discretized and written in the form of finite differences:

$$\begin{aligned} \frac{1}{D} \frac{\partial \rho_{i,j,k}}{\partial t} \approx \Psi & \left[\frac{(\rho_{i+1,j,k} - \rho_{i,j,k}) - (\rho_{i,j,k} - \rho_{i-1,j,k})}{\delta^2}, \right. \\ & \frac{(\rho_{i,j+1,k} - \rho_{i,j,k}) - (\rho_{i,j,k} - \rho_{i,j-1,k})}{\delta^2}, \\ & \frac{(\rho_{i,j,k+1} - \rho_{i,j,k}) - (\rho_{i,j,k} - \rho_{i,j,k-1})}{\delta^2}, \\ & \left. \frac{(\rho_{i+1,j,k} - \rho_{i,j,k})}{\delta}, \frac{(\rho_{i,j+1,k} - \rho_{i,j,k})}{\delta}, \frac{(\rho_{i,j,k+1} - \rho_{i,j,k})}{\delta}, \rho_{i,j,k} \right] \quad (19) \end{aligned}$$

In the limit of small δ , eq 19 turns into eq 18. However, we will assume that eq 19 is not only the numerical equivalent of eq 18 but also represents the physics behind eq 18. Namely, we assume that eq 19 describes the mass balance in an imaginary (i,j,k) network where fluxes from site to site are driven thermodynamically. In other words, there is an imaginary cubic lattice where molecules can sit on sites (i,j,k) , and $\rho_{i,j,k}$ is the probability of site (i,j,k) being occupied. Therefore, eq 19 can be written in the following form:¹⁹

$$\begin{aligned} \frac{1}{D} \frac{\partial \rho_{i,j,k}}{\partial t} \approx K & (f_{i+1,j,k}^+ - f_{i+1,j,k}^- + f_{i-1,j,k}^+ - f_{i-1,j,k}^- + f_{i,j+1,k}^+ - \\ & f_{i,j+1,k}^- + f_{i,j-1,k}^+ - f_{i,j-1,k}^- + f_{i,j,k+1}^+ - f_{i,j,k+1}^- + f_{i,j,k-1}^+ - f_{i,j,k-1}^-) \quad (20) \end{aligned}$$

where f^+ and f^- are fluxes coming into site (i,j,k) and coming out of site (i,j,k) , and K determines the units of the fluxes.

Note that viewing eq 19 as an equation for an imaginary lattice does not reduce our model to a lattice system, nor does the assumption of the finite difference form eq 19 for eq 18. However, considering eq 17 in the form eq 20 helps to find a functional form of operator ψ for interacting particles.

Fluxes $f_{i+1,j,k}^+$, $f_{i+1,j,k}^-$, $f_{i-1,j,k}^+$, and $f_{i-1,j,k}^-$ for eq 20 can be written in the following form:

$$f_{i+1,j,k}^+ = \frac{1}{z_0} \rho_{i+1,j,k} (1 - \rho_{i,j,k}) \lambda_{i,j,k} \quad (21)$$

$$f_{i+1,j,k}^- = \frac{1}{z_0} \rho_{i,j,k} (1 - \rho_{i+1,j,k}) \lambda_{i,j,k} \exp(H_{i,j,k} - H_{i+1,j,k}) \quad (22)$$

$$f_{i-1,j,k}^+ = \frac{1}{z_0} \rho_{i-1,j,k} (1 - \rho_{i,j,k}) \lambda_{i-1,j,k} \exp(H_{i-1,j,k} - H_{i,j,k}) \quad (23)$$

$$f_{i-1,j,k}^- = \frac{1}{z_0} \rho_{i,j,k} (1 - \rho_{i-1,j,k}) \lambda_{i-1,j,k} \quad (24)$$

where $\lambda_{i,j,k} = \min [1, \exp(H_{i+1,j,k} - H_{i,j,k})]$, and z_0 is the coordination number for the imaginary lattice ($= 6$ for a cubic lattice).

Note that the factor $\rho_{i+1,j,k} (1 - \rho_{i,j,k})$ in eq 21 is the probability of having a molecule on site $(i + 1, j, k)$ and site (i, j, k) being empty. Similar factors are in eqs 22–24. So, a molecule has a chance to move from site 1 to site 2 if it is available on site 1 and if site 2 is empty. The factor $1/z_0$ adjusts the probability of moving from site 1 for the number of neighboring sites. Factors $\exp(H_{i+1,j,k} - H_{i,j,k})$ in eqs 21–24 are Metropolis' probabilities of acceptance when a molecule moves up the energy gradient; these factors disappear when a molecule moves down the energy gradient.

To avoid cumbersome notation, consider the one-dimensional case that easily can be generalized for two and three dimensions. Plugging eqs 21–24 into the one-dimensional version of eq 20 gives:

$$\frac{1}{D} \frac{\partial \rho_i}{\partial t} \approx \frac{K}{z_0} [\rho_{i+1}(1 - \rho_i) \exp(H_{i+1} - H_i) - \rho_i(1 - \rho_{i+1}) + \rho_{i-1}(1 - \rho_i) - \rho_i(1 - \rho_{i-1}) \exp(H_i - H_{i-1})] \quad (25)$$

Consider the expansions:

$$\rho_{i+1} = \rho_i + \frac{\partial \rho_i}{\partial x} \delta + \frac{1}{2} \frac{\partial^2 \rho_i}{\partial x^2} \delta^2 + o(\delta^3) \quad (26)$$

$$\rho_{i-1} = \rho_i - \frac{\partial \rho_i}{\partial x} \delta + \frac{1}{2} \frac{\partial^2 \rho_i}{\partial x^2} \delta^2 + o(\delta^3) \quad (27)$$

$$H_{i+1} = H_i + \frac{\partial H_i}{\partial x} \delta + \frac{1}{2} \frac{\partial^2 H_i}{\partial x^2} \delta^2 + o(\delta^3) \quad (28)$$

$$H_{i-1} = H_i - \frac{\partial H_i}{\partial x} \delta + \frac{1}{2} \frac{\partial^2 H_i}{\partial x^2} \delta^2 + o(\delta^3) \quad (29)$$

where $\partial \rho_i / \partial x$ is $\partial \rho(x) / \partial x$ at $x = i$, $\partial^2 \rho_i / \partial x^2$ is $\partial^2 \rho(x) / \partial x^2$ at $x = i$, $\partial H_i / \partial x$ is $\partial H(x) / \partial x$ at $x = i$, and $\partial^2 H_i / \partial x^2$ is $\partial^2 H(x) / \partial x^2$ at $x = i$. Plugging ρ_{i+1} , ρ_{i-1} , H_{i+1} , and H_{i-1} from eqs 26–29 into eq 25 gives after algebraic manipulations:

$$\frac{1}{D} \frac{\partial \rho_i}{\partial t} \approx \frac{K}{z_0} \left[\frac{\partial^2 \rho_i}{\partial x^2} + (1 - 2\rho_i) \frac{\partial \rho_i}{\partial x} \frac{\partial H_i}{\partial x} + \rho_i(1 - \rho_i) \frac{\partial^2 H_i}{\partial x^2} \right] \delta^2 + o(\delta^3) \quad (30)$$

Note that the linear term (with respect to δ) cancels and the first meaningful term is quadratic; the symbol $o(\delta^3)$ denotes cubic and higher terms.

Comparison of eq 29 with eqs 17–19 indicates that $K = z_0 / \delta^2$ and the original continuous equation is

$$\frac{1}{D} \frac{\partial \rho}{\partial t} = \frac{\partial^2 \rho}{\partial x^2} + (1 - 2\rho) \frac{\partial \rho}{\partial x} \frac{\partial H}{\partial x} + \rho(1 - \rho) \frac{\partial^2 H}{\partial x^2} = \frac{\partial^2 \rho}{\partial x^2} + \frac{\partial}{\partial x} \left[\rho(1 - \rho) \frac{\partial H}{\partial x} \right] \quad (31)$$

where $\rho(1 - \rho) \partial H / \partial x$ is the “mobility” term. Generalization of eq 31 to a vector form and variable D gives

$$\partial \rho / \partial t = \nabla \{ D [\nabla \rho + \rho(1 - \rho) \nabla H] \} \quad (32)$$

coinciding with eq 3. Note that eqs 18–32 illustrate a possible logic in deriving a diffusion equation with a “mobility” term. More details and discussion on that can be found in refs 19–22.

References and Notes

- (1) Hill, T. *Statistical Mechanics*; McGraw-Hill: New York, 1956.
- (2) McQuarrie, D. A. *Statistical Mechanics*; Harper & Row: New York, 1976.
- (3) Croxton, C. A. *Liquid State Physics: A Statistical Mechanical Introduction*; Cambridge University Press: Cambridge, 1974.
- (4) Ornstein, L. S.; Zernike, F. *Proc. Acad. Sci. Amsterdam* **1914**, *17*, 793.
- (5) Rushbrooke, G. S. *Statistical Mechanics of Equilibrium and Nonequilibrium*; Meixner, J., Ed.; North-Holland Publishing: Amsterdam, 1965.
- (6) Rowlinson, J. S. *Rep. Prog. Phys.* **1965**, *28*, 169.
- (7) Frisch, H.; Lebowitz, J. L. *The Equilibrium Theory of Classical Fluids*; Benjamin: New York, 1964.
- (8) Percus, J. K.; Yevick, G. J. *Phys. Rev.* **1958**, *110*, 1.
- (9) Klein, M. *Phys. Fluids* **1964**, *7*, 391.
- (10) Boyer, D.; Tarjus, G.; Viot, P.; Talbot, J. J. *Chem. Phys.* **1995**, *104*, 1607.
- (11) Lazaridis, T.; Karplus, M. *J. Chem. Phys.* **1996**, *105*, 4294.
- (12) Stillinger, F. H.; Torquato, S.; Eroles, J. M.; Truskett, T. M. *J. Phys. Chem. B* **2001**, *105*, 6592.
- (13) Torquato, S.; Stillinger, F. H. *Phys. Rev. E* **2003**, *68*, 041113.
- (14) Savenko, S. V.; Dijkstra, M. *Phys. Rev. E* **2005**, *72*, 021202.
- (15) Aranovich, G. L.; Donohue, M. D. *Comput. Chem.* **1998**, *22*, 429.
- (16) Aranovich, G. L.; Donohue, M. D. *Phys. Rev. E* **1999**, *60*, 5552.
- (17) Bagchi, B.; Cerjan, C.; Rice, S. A. *Phys. Rev. B* **1983**, *28*, 6411; *J. Chem. Phys.* **1983**, *79*, 5595.
- (18) Kuespert, D. R.; Muralidharan, V.; Donohue, M. D. *Mol. Phys.* **1995**, *86*, 201.
- (19) Aranovich, G. L.; Donohue, M. D. *J. Phys. Chem. B* **2005**, *109*, 16062.
- (20) Giacomini, G.; Lebowitz, J. L. *Phys. Rev. Lett.* **1996**, *76*, 1094.
- (21) Giacomini, G.; Lebowitz, J. L. *J. Stat. Phys.* **1997**, *87*, 37.
- (22) Giacomini, G.; Lebowitz, J. L.; Marra, R. *Nonlinearity* **2000**, *13*, 2143.
- (23) Aranovich, G. L.; Donohue, M. D. *Physica A* **1997**, *242*, 409.
- (24) Aranovich, G. L.; Donohue, M. D. *Langmuir* **2003**, *19*, 2162; **2003**, *19*, 3822.
- (25) Aranovich, G. L.; Donohue, M. D. *J. Chem. Phys.* **2003**, *119*, 478.
- (26) Erickson, Aranovich, G. L.; Donohue, M. D. *Mol. Phys.* **2002**, *100*, 2121.
- (27) Ono, S.; Kondo, S. In *Encyclopedia of Physics*; Flugge, S., Ed.; Springer-Verlag: Berlin-Göttingen, 1960; Vol. 10, p 134.
- (28) Rowlinson, J. S.; Widom, B. *Molecular Theory of Capillarity*; Clarendon Press: Oxford, 1982; Section 5.3.
- (29) Widom, B. *J. Phys. Chem.* **1996**, *100*, 13190.
- (30) Carnahan, N. F.; Starling, K. E. *J. Chem. Phys.* **1969**, *51*, 635.
- (31) Lee, L. L. *Molecular Thermodynamics of Nonideal Fluids*; Butterworth Publishers: Boston, 1988; Chapter 6.
- (32) Hocker, T.; Aranovich, G. L.; Donohue, M. D. *J. Colloid Interface Sci.* **1999**, *211*, 61.